

# Povidone–iodine as a corrosion inhibitor towards a low modulus beta Ti-45Nb implant alloy in a simulated body fluid

S. M. Bhola · R. Bhola · B. Mishra ·  
D. L. Olson

Received: 30 March 2010 / Accepted: 21 February 2011 / Published online: 19 March 2011  
© Springer Science+Business Media, LLC 2011

**Abstract** Povidone-iodine and various bactericidal agents used in dental procedures may affect the corrosion response of an implant/prosthesis in the oral environment. The effect of various concentrations of povidone–iodine (PI) on the corrosion behavior of a low modulus beta titanium alloy, Ti-45Nb, has been investigated in normal saline solution. The open circuit potential, electrochemical impedance spectroscopy and potentiodynamic polarization measurements have been used to assess the electrochemical response of the alloy surface on PI addition so as to effectively predict the prosthetic treatment outcome. As the concentration of PI is increased, the corrosion rate decreases, suggested by decreased  $R_p$  values. Povidone–iodine acts as an anodic inhibitor by adsorbing on the anodic sites of the alloy. Addition of PI to a simulated body fluid such as normal saline leads to a decrease in corrosion rate of Ti-45Nb alloy.

## 1 Introduction

Povidone–iodine (PI) (Fig. 1) is a widely used antiseptic agent for various dental applications [1–9]. A prostheses or a newly inserted implant can get exposed to PI from minutes to days depending upon the therapy performed [10]. In our previous study, an attempt was made to understand the effect of PI addition to normal saline solution as a simulated body fluid on the corrosion behavior of commercially pure Ti-1 alloy [10]. Beta alloys are the potential alloys considered favorable for implant

applications over the alpha and mixed alloys. There have been various findings related to the effect of alloying elements on the strength and modulus of the beta Ti alloys [11] which suggest that Nb, Mo, Zr and Ta are suitable alloying elements for the beta Ti alloys, capable of enhancing the strength and reducing the modulus of these materials. Ti-45Nb alloy possesses a low elastic modulus (62 GPa) and also has the advantage of having only one alloying element (Nb) which has never been shown or suggested as having short-term or long-term potential adverse effect in the human body [12–14].

The aim of this investigation is to shed light on the effect of PI on the corrosion response of a low modulus beta Ti-45Nb alloy in normal saline solution.

## 2 Materials and methods

### 2.1 Materials preparation

Titanium alloy grade Ti-45Nb having composition (determined by optical emission spectrometry and shown in Table 1) as per ASTM standard [15] was used for the present investigation. Available cuboidal rod was cut to expose cross-section area of 0.85 cm<sup>2</sup> and mounted in epoxy resin for use as a working electrode. The exposed surface of specimens was finished with different grades of SiC grit papers (2400 grit max, polished over the diamond abrasive wheel (0.25 μm diamond paste) and finally washed with acetone.

Normal saline solution (sodium chloride inj, USP, HOSPIRA; composition: 5.26 g l<sup>-1</sup> sodium chloride, 2.22 g l<sup>-1</sup> anhy. sodium acetate, 5.02 g l<sup>-1</sup> sodium gluconate, 0.37 g l<sup>-1</sup> potassium chloride and 0.3 g l<sup>-1</sup> magnesium chloride hexahydrate) having pH 6.6 was used to carry out

S. M. Bhola (✉) · R. Bhola · B. Mishra · D. L. Olson  
Department of Metallurgical and Materials Engineering,  
Colorado School of Mines, Golden, CO 80401, USA  
e-mail: sbhola@mines.edu; malhotra.shaily@gmail.com

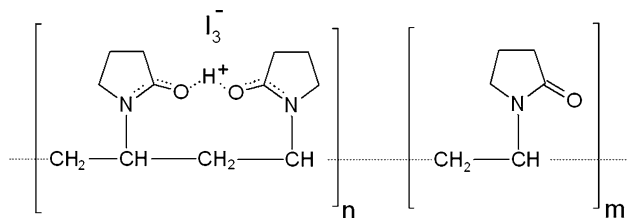


**Fig. 1** Structure of povidone-iodine

**Table 1** Chemical composition of Ti-45Nb as determined by OES

Composition (wt. %)						
C	H	N	O	Nb	Fe	Ti
0.04	0.0035	0.03	0.16	45.0	0.03	Bal

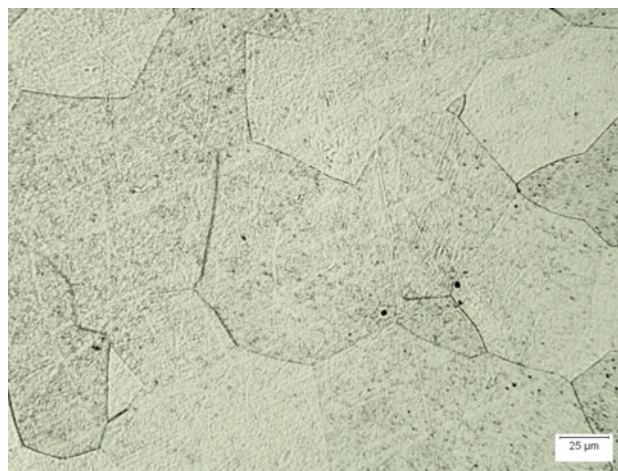


**Fig. 2** Microstructure of Ti-45Nb alloy

electrochemical testing of the alloy in pure normal saline and normal saline containing various PI concentrations. A 10% betadine solution (betadine solution, HOSPIRA) was used to prepare various concentrations such as 0.1, 0.2 and 1% in normal saline.

## 2.2 Measurements

For the microstructure determination, the alloy specimen was degreased, dried and mounted in bakelite resin. Mechanical grinding was done with SiC papers on a water cooled grinding stage up to paper 1800. Polishing was performed using gradually decreasing sizes of diamond abrasive from 6 to 1  $\mu\text{m}$  and finally using a fine grained  $\text{Al}_2\text{O}_3$  (with decreasing particle size from 0.5 to 0.25  $\mu\text{m}$ ) and cold saturated hydrous oxalic acid suspension on a short circular velvet cloth. The specimen was washed in de-ionized water and ethanol and air dried before etching. A universal etchant commonly known as the Kroll's reagent, a hydrous solution comprising of 2 ml HF (40% conc.) and 6 ml  $\text{HNO}_3$  (65% conc.) in 100 ml  $\text{H}_2\text{O}$  (de-ionized) was used for etching.

For the corrosion measurements, a three-electrode cell assembly consisting of Ti-45Nb alloy as the working electrode, platinum wire as the counter electrode and a saturated calomel electrode (SCE) as the reference electrode was used. Electrochemical testing was performed at 298 K under naturally aerated conditions in a closed system using a PAR potentiostat 273A and 1255 FRA.

Open circuit potential (OCP): OCP values were obtained at various immersion hours up to 48 h. for all the solutions.

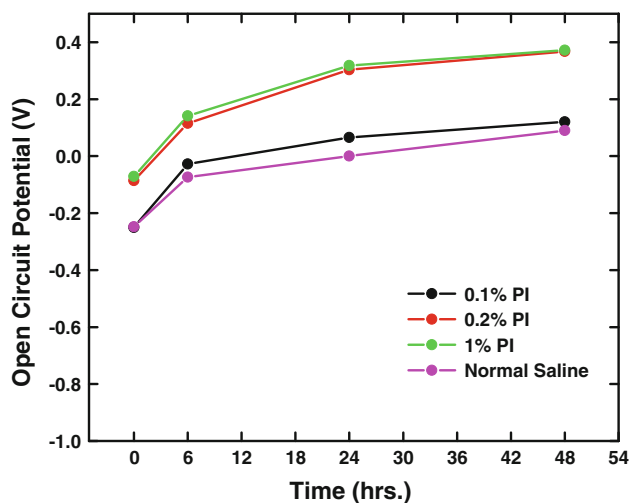


**Fig. 3** Open circuit potential as a function of time for Ti-45Nb alloy in normal saline and various concentrations of PI

Electrochemical impedance spectroscopy (EIS): Impedance measurements were performed using a PAR 1255 FRA at the OCP for various immersion hours such as 0, 6, 24 and 48. The frequency sweep was applied from  $10^5$  to  $10^{-1}$  Hz with the AC amplitude of 10 mV.

Potentiodynamic polarization: Potentiodynamic polarization measurements were performed at 48 h of immersion by polarizing the working electrode from an initial potential of  $-250$  mV versus OCP up to a final potential of 2 V versus SCE. A scan rate of 1 mV/s was used for the polarization sweep.

**Fig. 4** Circuit models used to fit EIS curves

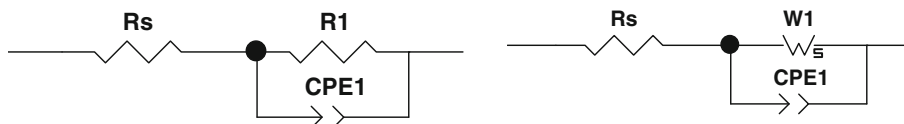
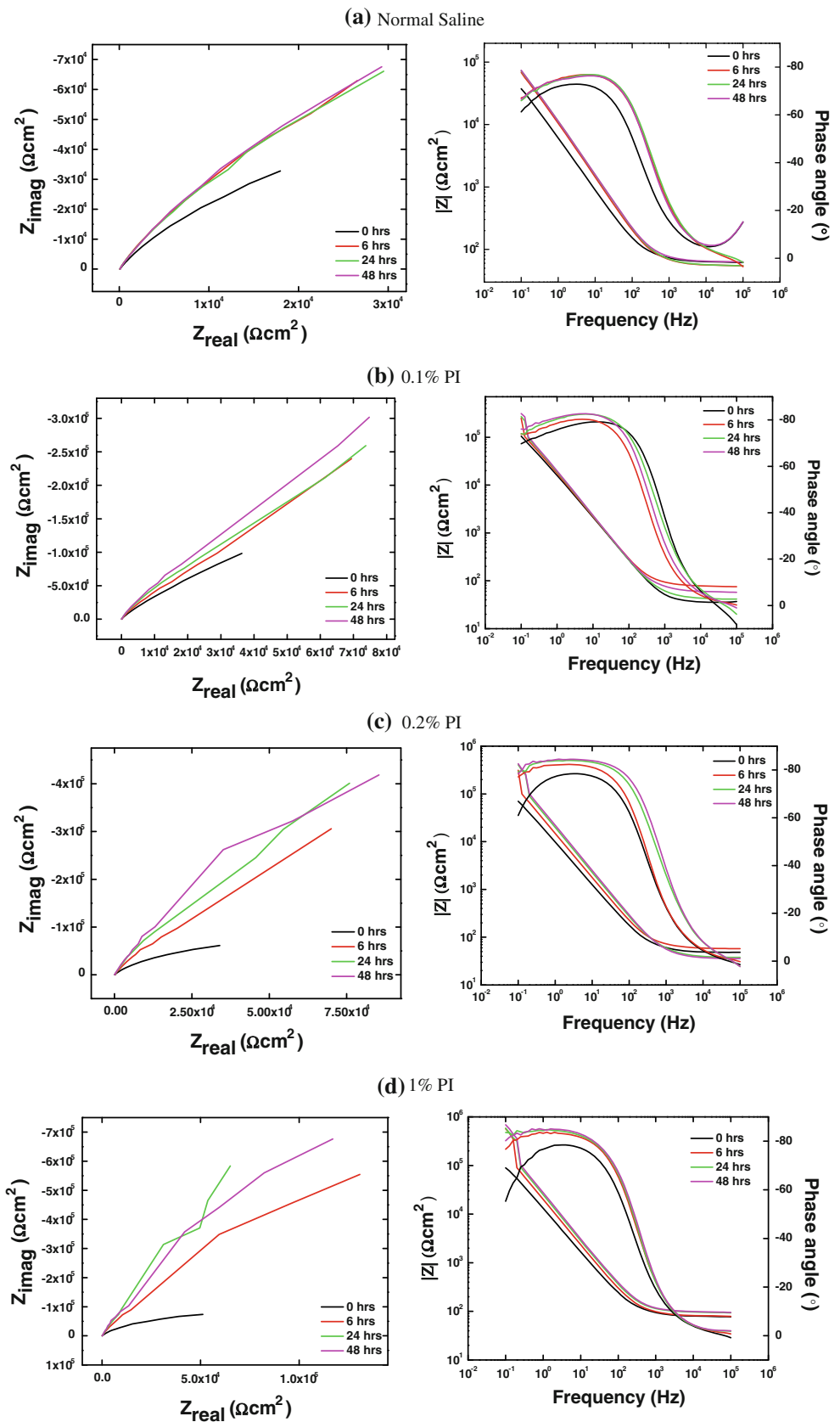


**Fig. 5** Impedance plots (Nyquist & Bode) for Ti-45Nb alloy in normal saline and various PI solutions at different immersion hours (a–d)



### 3 Results and discussion

Figure 2 presents the microstructure of Ti-45Nb alloy which primarily consists of large equiaxed grains of the beta phase. Minimal grain boundary precipitates are visible in the micrograph. The grain boundary lines and the pores are clearly visible after chemical etching. The grain size of the alloy is  $35 \pm 5 \mu\text{m}$ .

The average roughness of the alloy surface before performing the experiments was  $0.25 \pm 0.03 \mu\text{m}$ .

Figure 3 shows the variation of OCP with time for Ti-45Nb alloy in various PI solutions and normal saline. The OCP values increase with time for all cases which shows the stability of the passive oxide film in solution. The OCP values for 0.1, 0.2 and 1% solutions are more positive compared to normal saline. The OCP is the most noble for 1%, followed by 0.2 and 0.1%, in the decreasing order of PI concentrations. The increase in OCP on PI addition has been shown in our previous study [10].

The EIS curves for Ti-45Nb alloy in normal saline in the absence and presence of various concentrations of PI were found to fit the equivalent circuit models shown in Fig. 4, where  $R_s$  is the solution resistance,  $R_1$  is the charge transfer resistance ( $R_{ct}$ ),  $W_1$  is the Warburg impedance due to diffusion and CPE1 is the constant phase element for the capacitance of the passive oxide film. The impedance of the CPE is given by,

$$Z(\text{CPE}) = [Q(j\omega)^n]^{-1}$$

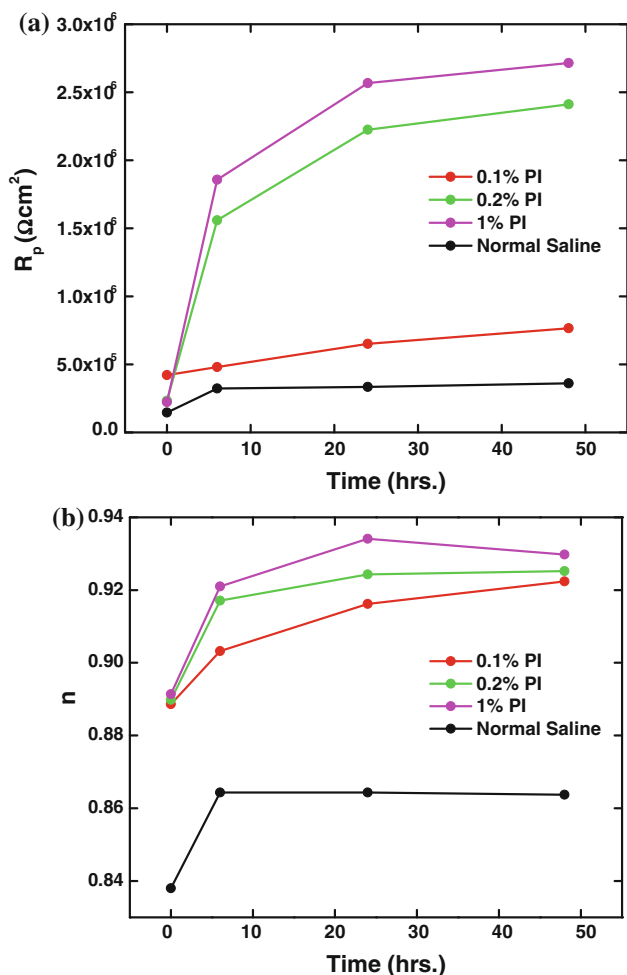
where  $Q$  is the constant of CPE,  $\omega$  is the angular frequency in  $\text{rad s}^{-1}$  and  $n$  is the exponential term which can vary between 1 for pure capacitance and 0 for a pure resistor [16].  $n$  is a measure of surface inhomogeneity, the lower is its value, the higher is the surface heterogeneity of the metal/alloy [17]. Diffusional impedance is characterized by three parameters,  $W(R)$ ,  $W(T)$  and  $W(P)$ .  $W(R)$  shows the length of diffusion impedance,  $W(T)$  is the diffusion time constant and  $W(P)$  is the phase factor,  $0 < W(P) < 1$ .

Figure 5 shows the impedance plots for Ti-45Nb in normal saline and various PI solutions at various immersion hours and the corresponding impedance parameters have been listed in Table 2. Figure 6 demonstrates the variation of polarization resistance (charge transfer or mass transfer) and the heterogeneity parameter,  $n$ , as a function of time.

From the nature of the Bode and Nyquist plots in Fig. 5, it can be noticed that there is an increase in the size of the Nyquist plots, an increase in impedance modulus in the modulus plots and increase in phase angle values towards the low frequency end with an increase in immersion time. The increase in  $R_p$  values with time for all solutions as observed in Fig. 5 and Table 2 correlates well with the increase in OCP values with increasing immersion hours. The increase in  $R_p$  with immersion time is, however,

**Table 2** Impedance parameters for Ti-45Nb alloy in normal saline and various PI solutions

Time (h)	$R_s$ ( $\Omega \text{ cm}^2$ )	$R_{ct}$ ( $\Omega \text{ cm}^2$ )	$Q$ $\text{S cm}^{-2} (\text{s rad}^{-1})^n$	$n$	$W_1\text{-R}$ ( $\Omega \text{ cm}^2$ )	$W_1\text{-T}$ (s)	$W_1\text{-P}$	Chi-square	Weighted sum of squares
Normal saline									
0	64.79	$1.45 \times 10^5$	$3.53 \times 10^{-5}$	0.8380	–	–	–	0.0028	0.35
6	56.26	$3.22 \times 10^5$	$1.83 \times 10^{-5}$	0.8643	–	–	–	0.0026	0.32
24	56.04	$3.34 \times 10^5$	$1.98 \times 10^{-5}$	0.8643	–	–	–	0.0028	0.35
48	63.93	$3.60 \times 10^5$	$1.83 \times 10^{-5}$	0.8637	–	–	–	0.011	1.43
0.1% PI									
0	35.04	$4.21 \times 10^5$	$1.23 \times 10^{-5}$	0.8886	–	–	–	0.0036	0.39
6	78.43	$4.80 \times 10^5$	$1.08 \times 10^{-5}$	0.9032	–	–	–	0.0028	0.30
24	43.29	$6.51 \times 10^5$	$9.94 \times 10^{-6}$	0.9162	–	–	–	0.0051	0.57
48	60.49	$7.66 \times 10^5$	$9.41 \times 10^{-6}$	0.9224	–	–	–	0.0047	0.52
0.2% PI									
0	49.69	$2.32 \times 10^5$	$1.95 \times 10^{-5}$	0.8898	–	–	–	0.0036	0.50
6	59.97	$1.55 \times 10^6$	$1.25 \times 10^{-5}$	0.9171	–	–	–	0.0048	0.55
24	40.07	–	$9.20 \times 10^{-6}$	0.9243	$2.22 \times 10^6$	0.52	0.87	0.0095	1.06
48	37.72	–	$5.41 \times 10^{-6}$	0.9252	$2.41 \times 10^6$	0.51	0.98	0.0054	0.60
1% PI									
0	80.98	$2.22 \times 10^5$	$1.46 \times 10^{-5}$	0.8914	–	–	–	0.0043	0.52
6	82.96	–	$9.10 \times 10^{-6}$	0.9210	$1.85 \times 10^6$	0.42	0.87	0.0051	0.57
24	99.87	–	$6.46 \times 10^{-6}$	0.9341	$2.56 \times 10^6$	0.53	0.87	0.0047	0.50
48	97.74	–	$7.24 \times 10^{-6}$	0.9298	$2.71 \times 10^6$	0.40	0.87	0.0058	0.62



**Fig. 6** Variation of **a**  $R_p$  and **b**  $n$  as a function of time for Ti-45Nb alloy in normal saline and various concentrations of PI

considerably lower in case of pure normal saline and 0.1% PI as compared to the other two higher PI concentrations as seen in Fig. 6a. In the intermediate to low frequency range, the phase angle values approach  $-90^\circ$  and the slope of the

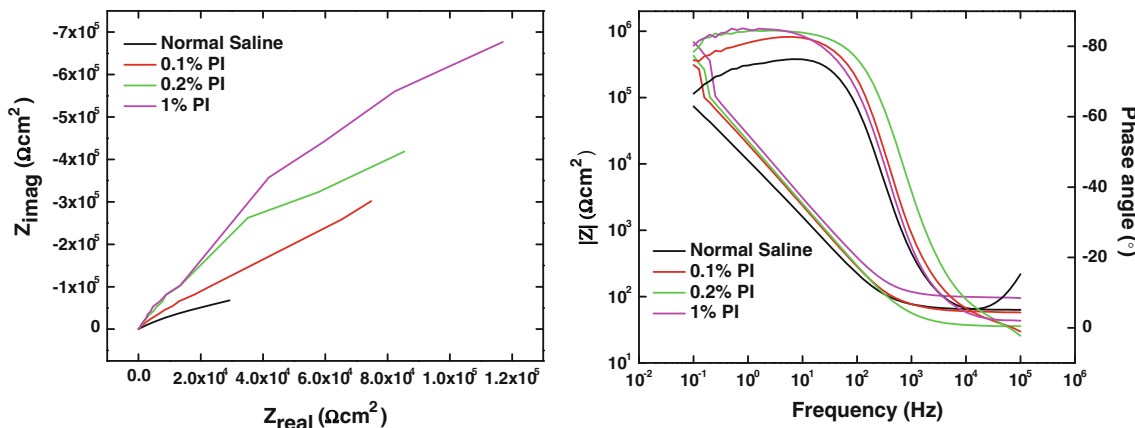
impedance modulus approaches  $-1$ , indicating a near-capacitive response of the oxide formed in solution.

On comparing the  $R_p$  values for various solutions at various immersion hours in Fig. 6a, it appears that the order of  $R_p$  is  $1\% > 0.2\% > 0.1\% > \text{normal saline}$ . Figure 7 compares the EIS plots for Ti-45Nb for normal saline and various concentrations of PI at 48 h of immersion. This observation clearly indicates an inhibition effect of PI on the corrosion behavior of Ti-45Nb alloy in normal saline solution. Moreover, as the concentration of PI is increased in normal saline, the efficiency of the inhibitor increases.

At higher concentrations of PI and at increasing immersion hours, the electrochemical reaction occurring at the alloy/oxide/adsorbed PI/solution interface becomes diffusion controlled due to an increased surface coverage of the alloy surface with PI molecules. This is clearly revealed as an increase in the  $W(R)$  values under these conditions. These results show that PI molecules adsorb on the alloy surface and act as a barrier towards electrochemical reactions occurring on the alloy surface and their corrosion inhibition effect increases with increasing concentrations of PI.

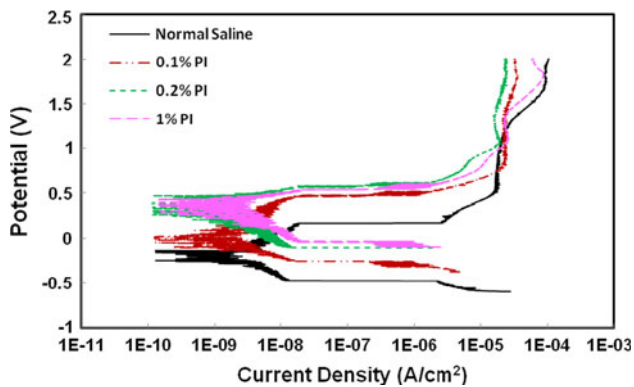
The variation in the heterogeneity parameter with immersion time in Fig. 6b for various solutions complements the results obtained above. The increase in the value of  $n$  with increasing PI concentrations and the lowest value for normal saline suggest the tendency of PI molecules to offer a better adsorption through a homogeneous distribution as the concentration is increased.

Figure 8 shows the potentiodynamic polarization curves for Ti-45Nb for normal saline and various PI concentrations at 48 h of immersion. In Fig. 8, it is observed that Ti-45Nb shows nobler corrosion potential values in solutions containing PI as compared to pure normal saline. For all concentrations of PI, the anodic current density has decreased as compared to pure normal



**Fig. 7** Impedance plots (Nyquist & Bode) for Ti-45Nb alloy in normal saline and various PI solutions at 48 h. of immersion





**Fig. 8** Potentiodynamic polarization curves for Ti-45Nb alloy in normal saline and various PI solutions at 48 h of immersion

saline. This shift has caused the corrosion potential to rise in the anodic direction. As discussed above, PI acts as an inhibitor towards the corrosion of Ti-45Nb alloy and its efficiency increases with increasing concentrations in the range of concentrations studied (0.1–1%). The shift in the corrosion potential in the anodic direction with a simultaneous lowering of the anodic currents further indicates that the inhibitor acts as an anodic inhibitor and slows down the metal dissolution reaction by adsorbing on the anodic sites of the alloy. This is possible through the interaction of the lone pair of electrons on nitrogen (N) and oxygen (O) or via a synergistic effect of iodide ions ( $I^-$ ) and protonated/positively charged PI molecules. Iodide ion is known for its inhibitive effect on metal surfaces by specific adsorption and further promoting the adsorption of organic cations by forming intermediate bridges between the positively charged metal surface and the positive end of the inhibitor [18].

In our previous study [10], PI concentrations in the same range from 0.1 to 1% in normal saline were investigated for commercially pure titanium (Ti-1) alloy. Only the lowest concentration showed an inhibition effect, while the higher concentrations increased the corrosion of Ti-1 alloy. The nature of the polarization curves in the presence of PI was, however, similar to the curves obtained for Ti-45Nb alloy. Adsorption is a complex phenomena which involves the interaction between the base electrolyte, substance under investigation (corrosion inhibitor or promoter) and the alloy surface. Corrosion inhibition can thus be very specific for an alloy, corrosive medium and the inhibitor. In addition, other studies have shown the efficacy of PI as an effective corrosion inhibitor for metals in acid solutions [18, 19]. Different bactericidal agents can have different effects on the implant-body fluid interface depending upon their chemical/electrochemical interaction with the alloy. Chlorhexidine gluconate, another bactericidal agent, has been shown to cause corrosion of titanium and stainless steel alloys [20, 21].

## 4 Conclusions

The EIS response of Ti-45Nb alloy in both normal saline and varying PI concentrations follows a one time constant circuit model, suggesting the formation of a single passive film on the alloy surface. As the concentration of PI is increased, the corrosion rate decreases, suggested by decreased  $R_p$  values. This indicates that in addition to imparting a bactericidal effect, PI addition also helps in preventing active corrosion of the prosthesis/implant in the oral cavity.

In addition, at increasing immersion hours, the concentrations of PI in the range examined, cause less implant deterioration, which might enhance the biological tissue response to a better treatment prognosis.

## References

- Demir A, Malkoc S, Sengun A, Koyuturk AE, Sener Y. Effects of chlorohexidine and povidone–iodine mouth rinses on the bond strength of an orthodontic composite. *Angle Orthod.* 2005;75(3): 392–6.
- Barabas EZ. *Vinylamines encyclopedia of polymer science and engineering*, vol. 17. 2nd ed. New York: Wiley; 1989. p. 219.
- Brittain HG. *Analytical profiles of drug substances and excipients*, vol. 22. San Diego: Academic Press; 1998. p. 25.
- Fuoss RM, Strauss VP. Viscosity of mixtures of polyelectrolytes and simple electrolytes. *Ann N Y Acad Sci.* 1949;51:836.
- LaRocca R, LaRocca M-AK, Ansell JM. Microbiology of povidone–iodine. In: Proc. Intl. Symp. On Povidone, Digenis GA, Ansell J, editors. University of Kentucky College of Pharmacy 1983; 101.
- Broussoulaux C. A New Antiseptic: Polyvinylpyrrolidone-Iodine, Dissertation submitted in partial fulfillment for the Doctorate of Medicine, University of Paris (France) 1965 (submitted).
- Cournoyer RF, Siggia S. Interaction of poly(vinyl-pyrrolidone) and iodine. *J Polym Sci.* 1974;12:603.
- Daniels WE, Chiddix ME, Glickman SA. Lactam complexes of Br–HBr. *J Org Chem.* 1963;28:573.
- Ferguson AW, Scott JA, McGavigan J, Elton RA, McLean J, Schmidt U, Kelkar R, Dhillon B. Comparison of 5% povidone–iodine solution against 0.1% povidone–iodine solution in preoperative cataract surgery antisepsis: a prospective randomized double blind study. *Br J Ophthalmol.* 2003;87:163–7.
- Bhola R, Bhola SM, Mishra B, Olson DL. Effect of povidone–iodine addition on the corrosion behavior of cp-Ti in normal saline. *J Mater Sci Mater Med.* 2010. doi:10.1007/s10856-010-4001-0.
- Chu PK, Chen JY, Wnag LP, Huang N. Plasma-surface modification of biomaterials. *Mater Sci Eng: R: Rep.* 2002;36(5–6): 143–206.
- Eisenbarth E, Velten D, Muller M, Thull R, Breme J. Biocompatibility of  $\beta$ -stabilizing elements of titanium alloys. *Biomaterials.* 2004;25:5705–13.
- Hanawa T. Metal ion release from metal implants. *Mater Sci Eng C.* 2004;24:745–52.
- Niinomi M. Fatigue performance and cyto-toxicity of low rigidity titanium alloy, Ti-29Nb-13Ta-4.6Zr. *Biomaterials.* 2003;24: 2673–83.

15. ASTM Standard F-04.12.44, ASTM International, Conshohocken, PA, USA.
16. Hsu CH, Mansfeld F. Technical note: concerning the conversion of the constant phase element parameter ( $Y_0$ ) into a capacitance. *Corrosion*. 2001;57:747–8.
17. Chongdar S, Gunasekaran G, Kumar P. Corrosion inhibition of mild steel by aerobic biofilm. *Electrochim Acta*. 2005;50:4655–65.
18. Umoren SA, Eduok UM, Oguzie EE. Corrosion inhibition of mild steel in 1 M  $H_2SO_4$  by polyvinyl pyrrolidone and synergistic iodide additives. *Portugaliae Electrochimica Acta*. 2008;26(6):533–46.
19. Umoren SA, Ebenso EE. Blends of polyvinyl pyrrolidone and polyacrylamide as corrosion inhibitors for aluminium in acidic medium. *Indian J Chem Technol*. 2008;15:355–63.
20. Öztan, MD, Akman AA, Zaimoglu L, Bilgic S. Corrosion rates of stainless steel files in different irrigating solutions. *Int Endod J*. 2002;35:655–9.
21. Bhola SM, Bhola R, Mishra B, Olson DL. An electrochemical study on chlorhexidine gluconate addition to normal saline for oral implant applications. *J Mater Sci: Mater Med* (submitted).